

Published in final edited form as:

Blood. 2009 April 16; 113(16): 3696–3705. doi:10.1182/blood-2008-09-176511.

T-Cell Receptor- and CD28-induced Vav1 activity is required for the accumulation of primed T cells into antigenic tissue

Rachel David¹, Liang Ma¹, Aleksandar Ivetic², Aya Takesono³, Anne J. Ridley^{3,4}, Jian-Guo Chai¹, Victor Tybulewicz⁵, and Federica M. Marelli-Berg¹

¹Department of Immunology, Division of Medicine, Imperial College London, Hammersmith Campus, London W12 ONN, UK

²BHF Cardiovascular Unit, National Heart and Lung Institute, Imperial College London, Hammersmith Campus, London W12 ONN, UK

³Ludwig Institute for Cancer Research, University College London, 91 Riding House Street, London W1W 7BS

⁵Division of Immune Cell Biology, National Institute for Medical Research, The Ridgeway, Mill Hill, London, NW7 1AA, UK

Abstract

Localization of primed T cells to antigenic tissue is essential for the development of effective immunity. Together with tissue-selective homing molecules, T-cell receptor (TCR)- and CD28-mediated signals have been shown to promote transendothelial migration of specific T cells into non-lymphoid antigen-rich tissue. However, the cellular and molecular requirements for T-cell accumulation to target tissue following their recruitment are largely undefined.

The guanine nucleotide exchange factor (GEF) Vav1 has an integral role in coupling TCR and CD28 to signalling pathways that regulate T cell activation and migration. Here, we have investigated the contribution of TCR- and CD28-induced Vav1 activity to the trafficking and localization of primed HY-specific CD4⁺ T cells to antigenic sites. Severe migratory defects displayed by Vav1^{-/-} T cells *in vitro* were fully compensated by a combination of shear flow and chemokines, leading to normal recruitment of Vav1^{-/-} T cells *in vivo*. In contrast, Vav1^{-/-} T-cell retention into antigen-rich tissue was severely impaired, reflecting their inability to engage in sustained TCR- and CD28-mediated interactions with tissue-resident antigen-presenting cells (APCs).

Correspondence to: Federica M. Marelli-Berg, Department of Immunology, Imperial College London, Hammersmith Hospital Campus, Du Cane Road, London W12 ONN, UK, Tel: +44(0)2083831704, Fax: +44(0)2083832788. f.marelli@imperial.ac.uk.

⁴Current address: King's College London, Randall Division of Cell and Molecular Biophysics, New Hunt's House, Guy's Campus, London SE1 1UL, UK

Authorship

RD: performed research and wrote the paper; LM: performed research; AI: designed and performed research; AT: performed research; AJR: designed research; VLT: designed research, contributed reagents; FM-B: designed research, wrote the paper.

The authors have no conflicting financial interests.

This novel function of APC-induced, TCR- and CD28-mediated Vav1 activity in the regulation of effector T-cell immunity highlights its potential as a therapeutic target in T-cell-mediated tissue damage.

Introduction

Following priming, specific T cells need to migrate and reside into antigenic sites where they are further re-activated and carry out their effector functions. Primed T-cell migration to non-lymphoid antigenic tissues is orchestrated by the expression of tissue-selective homing receptors by T cells which engage tissue-specific endothelial cell (EC) ligands 1. T-cell recruitment to target tissue is also induced by cognate recognition of antigen presented by EC surface major histocompatibility complex (MHC) 2–5 and by CD28 triggering 6 both *in vitro* and *in vivo*. Cognate recognition of resident conventional antigen-presenting cells (APCs) has been suggested to promote the selective accumulation of specific T cells into target tissue by delivering stop-signals and preventing them from leaving the tissue 7,8. The molecular mechanisms underlying the effects of T-cell receptor (TCR)- and CD28-triggering on T-cell migration and retention are at present only partially characterised 5, but they probably involve pathways conveying TCR and co-stimulatory-receptor signalling to the molecules that regulate adhesion and/or cytoskeletal rearrangements.

Vav1 is a 95KDa guanine nucleotide exchange factor (GEF) for Rho GTPases, which is present in cells of all haematopoietic lineages, including T cells. Vav1 has been found to have an important role in T-cell development 9–13, proliferation, interleukin-2 (IL-2) production and Ca²⁺ flux induction 12,14.

In addition, Vav1 regulates the cytoskeletal re-arrangements that are necessary for T-cell migration. For example, Vav1 controls integrin-mediated adhesion of thymocytes to extracellular matrix proteins 15,16. Vav1 has also been implicated in CXC-chemokine ligand 12 (CXCL12)-driven chemotaxis of T cells 17,18. The possibility that Vav1 activity mediates TCR and CD28-induced signalling that mediate T-cell motility has only been explored partially 15,16.

The involvement of Vav1-mediated signals in the regulation of T-cell localization to target tissue could explain recent findings showing that in experimental autoimmune encephalomyelitis 19, T cells from Vav1^{-/-} mice were significantly less able to infiltrate the brain compared with their wild type (WT) counterpart despite being activated, which led to decreased disease penetrance. Similarly, Vav1^{-/-} recipients of heart allografts displayed diminished graft infiltration by T cells, and this was associated with reduced rejection 20.

Based on this evidence, we have examined the contribution by Vav1-mediated signals to the constitutive, inflammation-induced and TCR/CD28-dependent primed T-cell recruitment and accumulation into antigenic tissue.

Methods

Mice

129sv male and female mice aged 7-9 weeks were purchased from Olac (Bicester, UK). Vav1^{-/-} mice were previously described 11. Procedures were carried out in accordance with the Home Office authority Act (1986).

Reagents, monoclonal antibodies (mAbs) and intravital dyes

The HY Dby peptide 21 was a gift from D. Scott. Mouse IFN γ was purchased from Peprotech. Golgi-plug was purchased from BD Pharmingen (Oxford, UK).

Anti-mouse CD4 was obtained from Caltag Laboratories (Burlingame, CA, USA). Anti-mouse CD69, CD25, CD62L were purchased from Cambridge biosciences (Cambridge, UK). All the other antibodies were purchased from BD Biosciences (Oxford, UK). The cell linker PKH26 and CFSE were purchased from Sigma-Aldrich (Gillingham, Dorset, UK). For labeling, the PKH26 and CFSE were added at a final concentration of 5 μ M and 1 μ M, respectively.

Cells

Mouse microvascular ECs were purified and cultured from mouse lung tissue as previously described 22. For functional assays the ECs were used between passage 4-6 and treated with 300 U/ml mouse IFN γ (PeproTech, London, UK) for 72 hours to induce MHC class II expression (data not shown) prior to use in experiments.

CD4⁺ WT and Vav1^{-/-} T cells specific for the male-specific minor histocompatibility antigen HY epitope Dby in the context of H2-A^b were obtained by two fortnightly ip immunisations of female Vav1^{-/-} mice or WT littermates with splenocytes (5x10⁸/mouse) from WT male littermates. Cells were maintained *in vitro* by fortnightly re-stimulation with irradiated (60Gy) male splenocytes (50x10⁶ splenocytes per 5x10⁶ T cells) and 20U/ml rIL2 (Roche, Hertfordshire UK) in T-cell medium (RPMI 1640 medium supplemented with 10% FCS (foetal-calf serum), 2 mM glutamine, 50 IU/mL penicillin, 50 μ g/mL streptomycin, 10mM HEPES and 50 mM 2-mercaptoethanol (ME). T-cell specificity was determined by ³HTdR incorporation and IFN γ production following **recognition of Dby peptide-pulsed female-derived splenocytes (Supplemental figure 1) and ECs (in the presence of non-mitogenic doses of rIL-2, data not shown)**. T cells were used 2 weeks after stimulation, following isolation on a Ficoll-Paque gradient, and incubation in medium alone overnight. The phenotype of T cells at the time of injection is shown in Supplemental Figure 2.

Bone marrow (BM)-derived DCs were obtained by flushing femurs from 7-10 week-old syngeneic female mice. BM cells (5 x 10⁶ /well) were seeded in a 6-well plate (Helena bioscience) in RPMI 1640 medium supplemented with 10% FCS, 2mM glutamine, 50 IU/mL penicillin, 50 μ g/mL streptomycin, 50 mM 2-ME and 8-16% murine granulocyte-macrophage colony stimulating factor (GM-CSF) obtained from the supernatant of the GM-CSF hybridoma (gift from A. George, Imperial College London). On days 3 and 5, fresh

culture medium was added to the plates. For functional assays, DCs were matured overnight with 100ng/ml LPS (Sigma) and used between 7-10 days post-isolation.

***In vitro* T-cell migration assays**—In adhesion assays, 96 well plates were coated with rICAM-1 (2µg/ml, R&D Systems Abingdon, UK) in Tris pH 8.5 for 2 hours at 37°C. Control wells were incubated with PBS alone. The plate was subsequently blocked with 2.5% bovine serum albumin (BSA) (Sigma) PBS at 37°C for 1 hour, and washed with 0.5% BSA. PHK26-labeled T cells were plated at 10³ /well and incubated for 10-60 minutes. T cells were washed once and the number of adherent cells was analysed with wide-field fluorescence microscopy. Control wells were not washed. The percentage adhesion was calculated with the following formula:

$$\frac{\text{Experimental adhesion} - \text{min adhesion}}{\text{Control adhesion} - \text{min adhesion}} \times 100$$

Control adhesion-min adhesion

The transwell assays were carried out using either plastic bound rICAM-1 or EC monolayers (2x10⁴ cells/well) on Transwell tissue-culture well inserts (diameter 6.5 mm) mounted with polycarbonate membranes with a 3µm pore size (Costar Ltd., High Wycombe, UK), as previously described 23. T cells (5 x10⁵/well) were added in each insert and left to migrate. The number of migrated T cells was determined by hemocytometric counting of the cells present in the well media at different time points over the next 24 hours. Results are expressed as percentage of transmigrated cells.

In time-lapse microscopy migration assays, 35mm dishes were coated with rICAM-1 in PBS and incubated at 4°C overnight. The plate was subsequently blocked with PBS containing 2.5% BSA at 37°C for 1 hour, and washed with 0.5% BSA/PBS. T cells were serum-starved in RPMI 2% FCS medium for 2 hours, seeded on the rICAM-1-coated dishes at a concentration of 1x10⁶/ml/dish and incubated at 37°C for 5-30min. Plates were washed once to remove non-adherent cells. T-cell migration was observed by time-lapse microscopy using Tempus software (Kinetic Imaging Ltd, Nottingham, UK). Images were acquired with a KPM1E/K-S10 CCD camera (Hitachi Denshi, Japan) using Kinetic Imaging software (Andor Technology, Belfast, UK) every 15-30 seconds for 25-50 minutes. The path of each cell was tracked for the whole of the time-lapse sequence using Tempus Meteor software (Andor Technology). Analysis of migration speed was then carried out using Mathematica 6.0 (Wolfram Research Institute) notebooks.

In chemotaxis assays, T cells were seeded (5-10x10⁵/well) in the upper chamber of a 5 µm-pore polycarbonate Transwell. A 0.5 ml volume of chemotaxis medium (RPMI 2% FCS) containing either CXCL10 (300ng/ml, Pepro Tech, Peterborough, UK) or CXCL12 (50ng/ml, PeproTech) was added to the bottom chamber, while 0.2 ml of cell suspension was added to the top chamber. Transwells were incubated for 6 hours at 37°C with 5% CO₂. The number of migrated cells was evaluated as described above.

Flow chamber assays

Male pulmonary ECs were grown to confluence in Nunc Slide Flaskettes (9 cm²; Nalge Nunc International, Denmark) that were pre-coated with fibronectin (10 µg/ml, Sigma); some cultures were stimulated for 48 hours with IFN γ (300U/ml), and in some experiments ECs were coated with CXCL10 (300ng/ml) for 2 hours prior to the assay. The flasks were then disassembled to use the slide for rolling assays. Slides were washed twice with PBS, 0.05% Tween 20 and mounted in a parallel-plate flow chamber (channel height 0.15 cm). The outer housing of the slide flaskette was removed and the remaining slide was mounted onto the flow chamber, which was maintained at a constant temperature of 37°C. WT and Vav^{-/-} T cells were perfused onto the flow chamber using a Harvard 2000 pump at a fixed shear stress of 2.5 dynes/cm². For a single experiment, a 20 ml mixture containing WT (green) and Vav^{-/-} (red) T-cells was perfused on the flow chamber at a final density of 2.5 x 10⁵ cells/ml. Perfusion of T cells was stopped at 17 minutes, and remaining non-adherent T cells were removed by perfusion of T-cell medium through the flow chamber for 2 minutes. The remaining 3ml of WT and Vav^{-/-} T-cell mixture was retained to determine the exact 'starting ratio' of the T-cell perfusion mixture using flow cytometry. Bound/transmigrated T-cells were harvested by removing the slide from the flow chamber and treating it with trypsin/EDTA. Ratios of red and green cells were calculated using flow cytometry, which was subsequently corrected against the value of the starting ratio in the perfusion mixture.

DC:lymphocyte conjugate formation assays

These experiments were carried out following a previously established protocol 15,16. Dby peptide-pulsed (50nM), CFSE-labeled female-derived DCs were used at 10⁵ DCs/condition. PKH26-labeled WT and Vav1^{-/-} T cells were used at 2.5x10⁵ cells/condition. DCs and T cells were spun at 650rpm for 5 minutes to increase the possibility of conjugate formation and co-incubated for 2 hours at 37°C. Conjugate formation was analysed by flow cytometry. T cells and DCs show a distinct pattern when analysed by FSC and SSC. Larger-sized cells (DCs) were gated and analysed for the presence of anti-CD4-APC positive T cells. Conjugate formation was analysed with flow cytometry and Flow Jo software.

Activation experiments

To induce stop signals, T cells were activated for 45 minutes with plate-bound 1µg/ml anti-CD3 and 5µg/ml anti-CD28 or 1µg/ml rat IgG and 5µg/ml hamster IgG as a control (Sigma) and subsequently stained for analysis. To induce CD28 signaling, the T cells were treated with a mixture of hamster anti-mouse CD28 (5µg/5x10⁶ cells), and rabbit anti-hamster Ig (2.5µg/5x10⁶ cells) for 30-45 minutes at 37 °C. As a control, T cells were treated with hamster Ig (5 µg/5x10⁶ cells) and rabbit anti-hamster Ig (2.5 µg/5x10⁶ cells).

Wide-field fluorescence microscopy and flow cytometry

Tissues were sampled and embedded in Optimal Cutting Temperature compound (OCT, Agar Scientific Ltd, UK), snap-frozen and stored until analysis. Peritoneal membranes or frozen tissue sections were laid onto Polysine Microscope slides (VWR International Lutterworth, Leicestershire, UK), left to dry overnight, and then mounted in Vectorshield mounting medium for fluorescence with DAPI (Vector Laboratories, Peterborough), to

visualize the nuclei (blue fluorescence). Slides were visualized with a Coolview 12-cooled CCD camera (Photonic Science, Newbury, UK) mounted over a Zeiss Axiovert S100 microscope equipped with Metamorph software (Zeiss, Welwyn Garden City, UK). A x10 and x40 NA 0.6 objectives and standard epi-illuminating fluoresceine and rhodamine fluorescence filter cube were used and 12bit image data sets were generated. Tissue infiltration was quantified by randomly selecting 6-10 10x-magnified fields and assessing the number of fluorescent cells in each field, as previously described 23. Quantification of T-cell infiltrates observed by wide-field fluorescence microscopy was performed using a specifically-designed software to run in the LabView (V7.1, National Instruments) environment. This automatic cell-counting algorithm is based on a combination of background subtraction, multiple thresholding and morphological processing approaches 6, which allows identifying single fluorescent cells in the tissue. The number of infiltrating cells obtained were then averaged and assessed statistically. Infiltration is expressed as the mean of fluorescent cells per 10x field in a given experimental condition \pm Standard Error.

DC:T cell interactions in tissues were also assessed by three-color analysis. Cell:cell contact (yellow fluorescence) is revealed by areas of overlapping membrane between CFSE-labeled DCs (green) and PKH26-labeled T cells (red). The mean number of DC: T-cell conjugates in 6-10 10x-magnified tissue samples was assessed by automatic cell counting. The data shown are based on the number of DCs engaged.

The presence of labeled cells in the peritoneal lavage was analysed by flow cytometry using a FACSCalibur (Becton Dickinson, Mountain View, CA) and FlowJo version 7.1.2 software (Tree Star Inc, Ashland, OR, USA).

Statistical analysis—In the *in vitro* experiments, comparisons between groups were made using the Student's t-Test. All reported p-values are two-sided.

Online Supplemental Material—The specificity and cytokine secretion by WT and Vav1^{-/-} T cells is described in Supplemental Figure 1. Supplemental Figure 2 shows the phenotype of WT and Vav1^{-/-} T cells. The upregulation of activation markers by WT and Vav1^{-/-} T cells is shown in Supplemental Figure 3. Supplemental Videos 1-2 display the characteristic of WT and Vav1^{-/-} T cells on ICAM-1, as observed by time-lapse microscopy.

Results

Constitutive and chemokine-induced Vav1^{-/-} T-cell migration is severely impaired *in vitro*, but preserved *in vivo*

HY(Dby)-specific A^b-restricted CD4⁺ memory T cells were generated by intraperitoneal (ip) immunization of Vav1^{-/-} female mice and WT littermates with male splenocytes, as previously described 5. WT and Vav1^{-/-} T cells displayed similar specificity, phenotypic and functional characteristics (Supplemental Figures 1-3), although functional responses, such as proliferation and interferon- γ (IFN γ) secretion by Vav1^{-/-} T cells were reduced compared with their WT counterpart.

Numerous phenotypic and functional defects were revealed by *in vitro* experiments that analysed the migratory ability of Vav1^{-/-} T cells, including decreased LFA-1 expression (Figure 1, panel A) adhesion and migration to ICAM-1 (B-C, E-F) and through endothelial cells (D), impaired de-adhesion and retraction of the uropode (Supplemental Videos 1 and 2) and significantly decreased response to chemokines (G).

To establish whether the severe migratory defects observed in Vav1^{-/-} T cells *in vitro* were reflected in altered constitutive trafficking *in vivo*, labeled HY-specific H2D^b-restricted CD4⁺ WT and Vav1^{-/-} T cells (10^7) were injected intravenously (iv) into female WT mice and their localization to the liver, kidney, lung and spleen was quantified 2, 6 and 24 hours post-injection by wide-field fluorescence microscopy.

Although higher numbers of WT T cells were found in the spleen and lung of recipients 2 hours post-injection, there was no significant difference in the number of WT and Vav1^{-/-} T cells which localized in all the tissues at all the other time points, suggesting that constitutive trafficking of primed Vav1^{-/-} T cells is not severely impaired *in vivo* (Figure 2-A).

In parallel, the recruitment of i.v. injected labeled HY-specific CD4⁺ WT and Vav1^{-/-} T cells to the peritoneal cavity in response to the inflammatory chemokine CXCL10 (IP-10) injected ip into syngeneic female mice was compared. In contrast to what we had observed *in vitro*, CXCL10 induced equal migration of WT and Vav1^{-/-} T cells to the peritoneal cavity (Figure 2-B and C). Owing to the presence of an autofluorescent population of non-T cells that is often detected in FL-2, cells were double-stained with an APC-conjugated anti-CD4 antibody following harvesting, and the percentage of PKH26 (FL-2)-labeled T cells gated in the CD4⁺ T-cell population is shown. These results suggest that T cells lacking Vav1 activity undergo normal trafficking in response to constitutive or non-specific inflammatory stimuli *in vivo* despite displaying defective migration *in vitro*.

Vav1^{-/-} T cells are recruited to-, but not retained into antigenic tissue—Previous reports (also by our group) have shown that the TCR engagement by antigen-presenting endothelium enhances specific T-cell migration and contributes to the recruitment of specific T cells to target tissue 2–5. Given that Vav1 activity is induced by TCR-triggering and is involved in the regulation of cytoskeletal reorganisation, we examined the possibility that Vav1^{-/-} T cells have a defect in TCR-driven migration.

Antigen-induced migration of HY-specific CD4⁺ H2A^b-restricted WT and Vav1^{-/-} T cells ($3\text{--}5 \times 10^5$) through IFN γ -treated antigenic (male) and non-antigenic (female) syngeneic EC monolayers was first compared. As expected, WT T cells showed increased migration through male-derived EC (Figure 3-A). In contrast, Vav1^{-/-} T cells showed reduced and comparable levels of migration through both male and female ECs. Similar observations were made when TCR-driven migration of HY-specific CD4⁺ H2A^b-restricted WT and Vav1^{-/-} T cells was examined by time-lapse microscopy (Figure 3-B).

To assess whether this defect was reflected in impaired antigen-dependent T-cell recruitment *in vivo*, HY-specific WT (PKH26-labeled) and Vav1^{-/-} (CFSE-labeled) T cells were co-injected iv in male and female mice (10^7 /mouse) that had previously **received an optimal**

dose of IFN γ ip to induce local up-regulation of MHC molecules by the microvessels and HY antigen presentation, as we have previously described 4,5. WT T cells were recruited in the membrane and some migrated to the peritoneal cavity of male but not female mice (Figure 3C-D). In contrast, Vav1 $^{-/-}$ T cells were not retained into the antigenic peritoneal tissue (Figure 3E-F), although they were readily detectable in the peritoneal cavity of male mice (Figure 3D). As expected, neither WT nor Vav1 $^{-/-}$ T cells reached the peritoneal membrane or cavity of female mice (Figure 3 D-F). These data suggest that, although HY-specific CD4 $^{+}$ Vav1 $^{-/-}$ T cells can be efficiently recruited to the site of antigen presentation, they are not retained in the antigenic tissue (the peritoneal membrane).

A combination of flow and chemokines compensates for the lack of Vav1 activity during T-cell recruitment *in vivo*

The discrepancy between defective migration by Vav1 $^{-/-}$ T cells *in vitro* and their normal recruitment *in vivo* suggests that additional, Vav1-independent mechanisms are in place to compensate for the loss of Vav1 activity *in vivo*. Shear flow and chemokine-induced signals have been shown to provide essential stimuli for the recruitment of T cells in physiological settings 24, including following cognate recognition of the endothelium 25,26. To address this possibility, we used a previously described model of antigen-dependent tissue infiltration *in vivo* in static conditions 23. In this model, HY-specific CD4 $^{+}$ H2A b -restricted WT and Vav1 $^{-/-}$ T cells (2×10^6) are injected ip into syngeneic male and female mice that had previously received an optimal dose of IFN γ ip (to induce local antigen presentation) and therefore T-cell recruitment in the peritoneal membrane occurs in the absence of shear flow. HY-specific WT T cells were promptly recruited to the peritoneal membrane and depleted from the peritoneal cavity of male, but not female, mice (Figure 4, panels A-B). In contrast, Vav1 $^{-/-}$ T cells failed to migrate to the peritoneal membrane of antigen-expressing male mice and remained localized in the peritoneal cavity. These data suggest that antigen-dependent cell:cell interactions leading to Vav1 $^{-/-}$ T-cell migration is impaired in static condition *in vivo*.

Prompted by these observations, we then sought to investigate whether exposure to shear flow and/or other stimuli could compensate for the migratory defects displayed by Vav1 $^{-/-}$ T cells *in vitro*. HY-specific CD4 $^{+}$ WT (PKH26-labeled) and Vav1 $^{-/-}$ T cells were perfused over untreated or IFN γ -treated (antigen-presenting) male-derived EC monolayers 24. As shown in Figure 4 C, WT T cells displayed a **5-fold increase in the recruitment through IFN γ -treated male-derived ECs**, whereas Vav1 $^{-/-}$ T cells still displayed defective migration, which was not increased in the presence of shear flow. As chemokine-mediated signals have been shown to co-operate with flow in the recruitment of T cells 24, we carried out further experiments in which untreated and IFN γ -treated male-derived EC monolayers were exposed to CXCL10 (300ng/ml) for 2 hours prior to use in the flow chamber assays. This led to increased and quantitatively similar recruitment of both WT and Vav1 $^{-/-}$ T cells irrespectively of antigen presentation. As experiments of similar design did not rescue T-cell migration in static transwell-based assays *in vitro* (data not shown), this suggests that a combination of shear flow and chemokine stimulation can rescue Vav1 $^{-/-}$ T-cell recruitment independently of antigen presentation by the endothelium.

Vav1^{-/-} T cells are not susceptible to ‘stop signals’ *in vitro* and *in vivo*—

Retention of specific T cells into non-lymphoid antigenic tissue has been thought to require their interaction with resident conventional (i.e. B7-expressing) APCs 7,8. The observation that memory Vav1^{-/-} T cells were efficiently recruited to antigenic sites but were not retained in the antigenic tissue prompted us to investigate the ability of Vav1^{-/-} T cells to establish sustained interactions with conventional tissue-resident APCs. To address this issue, the following approaches were taken.

First, we compared the ability of primed HY-specific CD4⁺ H2A^b-restricted WT and Vav1^{-/-} T cells ($3\text{-}5 \times 10^5$), which had previously undergone CD3 and CD28 antibody-mediated co-ligation (45 minutes at 37⁰C), to migrate through rICAM-1-coated transwells for 24 hours. The doses of CD3 and CD28 elicited similar levels of proliferation by WT and Vav1^{-/-} T cells (data not shown). HY-specific activated WT T cells migrated significantly less compared with those exposed to isotype control antibodies or medium alone (Figure 5, panel A). **As previously observed (See Figure 1), the baseline migration of Vav1^{-/-} T cells was far less efficient than that of their WT counterpart. In addition, migration of CD3/CD28-activated Vav1^{-/-} T cells was unchanged, suggesting that these cells are not susceptible to ‘stop signals’ *in vitro*.**

We then compared the ability of WT and Vav1^{-/-} HY-specific memory T cells to form conjugates with syngeneic dendritic cells (DCs). HY-specific CD4⁺ H2A^b-restricted WT and Vav1^{-/-} T cells (2.5×10^5) were labeled with PKH26 and incubated with lipopolysaccharide (LPS)-matured, Carboxyfluorescein succinimidyl ester (CFSE) -labeled female DCs (10^5) that were either untreated or pre-loaded with the cognate HY Dby peptide (50 nM). The dose of peptide was chosen based on its ability to induce similar levels of proliferation by WT and Vav1^{-/-} T cells (Supplemental figure 3). As expected, a higher percentage of HY specific WT T cells engaged Dby peptide-pulsed female DCs compared with non-antigenic syngeneic DCs (Figure 5 B-C). In contrast, antigen presentation did not enhance conjugate formation by Vav1^{-/-} T cells, in line with previous findings in immature and naïve T cells 15,16.

Finally, we investigated the interactions by HY-specific CD4⁺ H2A^b-restricted WT and Vav1^{-/-} T cells with tissue-resident conventional APCs *in vivo*. LPS-matured CFSE-labeled Dby peptide-pulsed (50nM) female DCs were injected ip in female mice (2×10^6 /mouse), followed by iv injection of PKH26 labeled HY-specific CD4⁺ WT or Vav1^{-/-} T cells (10^7 /mouse). As a control, non-antigenic DCs were also injected in some T-cell recipients. Also, some mice received T cells or Dby-pulsed or non-antigenic DCs alone. **A schematic representation of the trafficking patterns of iv-injected T cells and ip-injected DCs is provided for clarity in Supplemental Figure 4.** The presence of interacting labeled T cell and DCs in the peritoneal tissue and the spleen of recipient mice was analysed 24 hours later. Yellow fluorescence was apparent in the areas of cell:cell contact as a result of the interacting red-labeled T cells and Green-labeled DCs. As expected, a significantly higher number of DC:T cell conjugates were observed in the peritoneal membrane in mice injected with female DCs pre-pulsed with Dby peptide (Figure 6A) compared with non-antigenic DCs. This effect was not seen with Vav1^{-/-} T cells. Furthermore, numerous WT T cells that were not engaged by DCs were detected in the peritoneal membrane (compared with Vav1^{-/-}

T cells) of mice injected with peptide-pulsed DCs (Figure 6B), suggesting that WT specific T cells are temporarily retained in the target tissue following a previous encounter with antigen-presenting DCs, which has been described in lymphoid tissue 27. In addition, a lower number of labeled T cells was retrieved in the peritoneal cavity of recipients of HY-specific WT T cells and peptide-loaded DCs compared with recipients of WT T cells and non-antigenic DCs or Vav1^{-/-} T cells plus antigenic DCs or non-peptide-loaded DCs (Figure 6C), suggesting that T cells that had not engaged with antigenic DCs did not remain into the peritoneal tissue and migrated to the peritoneal cavity.

In line with these observations, a significantly higher percentage of T cell:DC conjugates was detected in the spleen of recipient mice that had received Dby peptide-loaded DCs and WT T cells than Vav1^{-/-} T cells (Figure 6D), confirming that Vav1 activity is required for the delivery of stop signals to trafficking T cells following cognate interactions with resident APCs, which leads to their accumulation into antigen-rich tissue.

Vav1^{-/-} T-cell motility is not susceptible to CD28-mediated regulation—Our results suggest that Vav1 activity is dispensable for T-cell recruitment by antigen-presenting ECs but is instrumental for their retention into target tissue, possibly following interactions with resident conventional APCs. A prominent feature of fully mature conventional APCs is the high expression of CD28 ligands, which is not observed in other parenchymal cells. We have recently reported that CD28 triggering promotes interactions with antigen-presenting cells by inducing integrin clustering and it is required for the localization of primed T cells to non-lymphoid antigen-rich tissue 6. As Vav1 can be activated by CD28 signals 28,29, we sought to assess the effect of CD28-induced Vav-1 activity on T-cell trafficking (in the absence of- or concomitant to- TCR-triggering).

HY-specific CD4⁺ H2A^b-restricted WT and Vav1^{-/-} T cells were pre-treated with a mixture of hamster anti-mouse CD28 and rabbit anti-hamster Ig and labeled with PKH26 prior to iv injection into female mice. As a control, T cells that had been treated with hamster Ig and rabbit anti-hamster Ig and labeled with CFSE were co-injected. Localisation to non-lymphoid tissue by T cells was assessed 24 hours post-injection. As previously described, CD28-stimulated WT T cells showed increased trafficking to kidney, lung, liver and spleen compared with the controls (Figure 7A). In contrast, HY-specific Vav1^{-/-} T cell infiltration of the same tissues was unaffected by CD28 triggering. This was somehow surprising, as TCR-dependent recruitment was not affected by Vav1 activity *in vivo*.

As in physiologic settings CD28 triggering is delivered in conjunction with TCR-engagement, the ability of CD28-mediated Vav1^{-/-} activity to enhance T-cell localization to target tissue in conjunction with TCR-mediated signals was also analysed. HY-specific CD4⁺ H2A^b-restricted WT and Vav1^{-/-} T cells were pre-treated with a mixture of hamster anti-mouse CD28 and rabbit anti-hamster Ig and labeled with PKH26 prior to iv injection into male mice that had previously received an optimal dose of IFN γ to induce local antigen presentation in the peritoneal tissue (Figure 7, B-C). CD28-activated WT T cells showed increased localization to the peritoneal membrane, but this effect was not observed with the Vav1^{-/-} T cells (5B). Similarly, CD28 triggering did not increase Vav1^{-/-} T-cell

accumulation into the peritoneal cavity (5C). These data suggest that in the absence of Vav1, CD28-mediated regulation of T-cell trafficking and tissue localization is impaired.

Discussion

It is becoming increasingly clear that TCR and CD28 co-engagement not only sustains the differentiation, expansion and development of effector function of T cells, but also optimizes the efficiency of the immune response by coordinating its anatomy 30. Recognition of antigen displayed by ECs directs T-cell extravasation to antigenic sites, by facilitating specific T-cell access 2–5. The cellular and molecular mechanisms that subsequently sustain T-cell retention in antigenic non-lymphoid tissue are less well understood. As a prominent role in mediating T-cell arrest has been ascribed to antigen-receptor engagement, it is likely that parenchymal APCs have a major role in this effect 7,8,31.

Several reports indicate that the GEF factor Vav1 is a key mediator in the transduction of TCR and CD28-mediated signals to the cytoskeleton, owing to its ability to activate Rho GTPases 15,16,28,29.

Despite Vav1^{-/-} T adhesion and chemotactic responses, and antigen-induced migration were severely compromised *in vitro*, constitutive and antigen-induced recruitment of primed Vav1^{-/-} T-cell was unaffected *in vivo*, due to compensatory mechanisms mediated by shear flow in conjunction with endothelium-displayed chemokines. We have recently reported that loss of TCR-induced PI3K p110 δ activity completely abrogated specific T cell recruitment to target tissue 32. Although both molecules are activated by TCR triggering, and can influence each other's activity, it is possible that p110 δ activity may be co-engaged by signalling pathways co-operating with the TCR in the regulation of T cell migration. In this context, it has recently been shown that that a ZAP-70-mediated chemokine-TCR cross talk is required to induce T-cell migration 17.

Despite being dispensable for primed T-cell recruitment to antigenic non-lymphoid tissue *in vivo*, Vav1 activity was required for T-cell infiltration and retention in shear-free microenvironment as, recruited Vav1-deficient T cells failed to accumulate in target tissue and continued to migrate. Similar to what has been described in lymph nodes 27, retention of specific T cells in non-lymphoid antigenic tissue is presumably mediated by cognate interactions with conventional resident APCs 7,8 and can be independent from chemokine-induced integrin activation 33, while requiring distinct additional signals. The observation that CD28 triggering of Vav1^{-/-} T cells does not promote their localization to non-lymphoid tissue is consistent with a co-operation between TCR- and CD28-mediated signals in the regulation of T cell motility. The contribution of CD28-mediated signals to the establishment of T cell:APC interactions sustaining T-cell localization to target tissue has been suggested by several studies 7,8. Reduced T-cell infiltrates are also commonly observed in B7-deficient target tissue despite efficient T- cell activation 34,35. Importantly, specific inhibition of the Vav1/Rac1 interaction upon CD28 signaling in human CD4⁺ T cells resulted in reduced lamellipodia formation and inhibition of the T cell:APC conjugate formation 36,37.

We propose that two mechanisms are likely to contribute to this effect. First, Vav1 activity is needed for T cell:APC cognate interactions in static conditions such as in parenchymal tissue. Second, retention of T-cell in the tissue may require additional signals that are delivered concomitantly to TCR triggering and that also require Vav1 activity. Based on the evidence presented here, TCR triggering by B7-deficient parenchymal cells, such as the mesothelium or stromal cells (in which MHC molecule upregulation is induced by IFN γ 4), is not enough to sustain specific Vav1^{-/-} T-cell retention. The observation that Vav1^{-/-} T cells are not susceptible to CD28-mediated regulation of T cell migration suggests that additional CD28-induced, Vav1-mediated signals may be necessary to allow this effect.

From a clinical perspective, given the recent reports of the effectiveness of pharmacological inhibition of Vav1 activity in autoimmunity and transplantation 36,37, our observations provide a molecular platform for pharmacologic targeting of Vav1 in the control of T-cell-mediated inflammation.

Supplementary Material

Refer to Web version on PubMed Central for supplementary material.

Acknowledgements

We are grateful to F. Vianello and K. Okkenhaug for critical review of the manuscript. R.D. was supported by a British Heart Foundation Scholarship (BHF PG/05/136/19997).

References

1. Mora JR, von Andrian UH. T-cell homing specificity and plasticity: new concepts and future challenges. *Trends Immunol.* 2006; 27:235–243. [PubMed: 16580261]
2. Savinov AY, Wong FS, Stonebraker AC, Chervonsky AV. Presentation of antigen by endothelial cells and chemoattraction are required for homing of insulin-specific CD8⁺ T cells. *J Exp Med.* 2003; 197:643–656. [PubMed: 12615905]
3. Greening JE, Tree TI, Kotowicz KT, et al. Processing and presentation of the islet autoantigen GAD by vascular endothelial cells promotes transmigration of autoreactive T-cells. *Diabetes.* 2003; 52:717–725. [PubMed: 12606513]
4. Marelli-Berg FM, James MJ, Dangerfield J, et al. Cognate recognition of the endothelium induces HY-specific CD8⁺ T-lymphocyte transendothelial migration (diapedesis) in vivo. *Blood.* 2004; 103:3111–3116. [PubMed: 15070692]
5. Jarmin SJ, David R, Ma L, et al. T cell receptor-induced phosphoinositide-3-kinase p110delta activity is required for T cell localization to antigenic tissue in mice. *J Clin Invest.* 2008; 118:1154–1164. [PubMed: 18259608]
6. Mirenda V, Jarmin SJ, David R, et al. Physiologic and aberrant regulation of memory T-cell trafficking by the costimulatory molecule CD28. *Blood.* 2007; 109:2968–2977. [PubMed: 17119120]
7. McGavern DB, Christen U, Oldstone MB. Molecular anatomy of antigen-specific CD8(+) T cell engagement and synapse formation in vivo. *Nat Immunol.* 2002; 3:918–925. [PubMed: 12352968]
8. Kawakami N, Nägerl UV, Odoardi F, Bonhoeffer T, Wekerle H, Flügel A. Live imaging of effector cell trafficking and autoantigen recognition within the unfolding autoimmune encephalomyelitis lesion. *J Exp Med.* 2005; 201:1805–1814. [PubMed: 15939794]
9. Fischer KD, Zmuldzinas A, Gardner S, Barbacid M, Bernstein A, Gidos C. Defective T-cell receptor signalling and positive selection of Vav-deficient CD4⁺ CD8⁺ thymocytes. *Nature.* 1995; 374:474–477. [PubMed: 7700360]

10. Tarakhovskiy A, Turner M, Schaal S, et al. Defective antigen receptor-mediated proliferation of B and T cells in the absence of Vav. *Nature*. 1995; 374:467–470. [PubMed: 7700358]
11. Turner M, Mee PJ, Walters AE, et al. A requirement for the Rho-family GTP exchange factor Vav in positive and negative selection of thymocytes. *Immunity*. 1997; 7:451–460. [PubMed: 9354466]
12. Fischer KD, Kong YY, Nishina H, et al. Vav is a regulator of cytoskeletal reorganization mediated by the T-cell receptor. *Curr Biol*. 1998; 8:554–562. [PubMed: 9601639]
13. Tybulewicz VL, Ardouin L, Prisco A, Reynolds LF. Vav1: a key signal transducer downstream of the TCR. *Immunol Rev*. 2003; 192:42–52. [PubMed: 12670394]
14. Costello PS, Walters AE, Mee PJ, et al. The Rho-family GTP exchange factor Vav is a critical transducer of T cell receptor signals to the calcium, ERK, and NF-kappaB pathways. *Proc Natl Acad Sci U S A*. 1999; 96:3035–3040. [PubMed: 10077632]
15. Krawczyk C, Oliveira-dos-Santos A, Sasaki T, et al. Vav1 controls integrin clustering and MHC/peptide-specific cell adhesion to antigen-presenting cells. *Immunity*. 2002; 16:331–343. [PubMed: 11911819]
16. Ardouin L, Bracke M, Mathiot A, et al. Vav1 transduces TCR signals required for LFA-1 function and cell polarization at the immunological synapse. *Eur J Immunol*. 2003; 33:790–797. [PubMed: 12616499]
17. Ticchioni M, Charvet C, Noraz N, et al. Signaling through ZAP-70 is required for CXCL12-mediated T-cell transendothelial migration. *Blood*. 2002; 99:3111–3118. [PubMed: 11964272]
18. Garcia-Bernal D, Wright N, Sotillo-Mallo E, et al. Vav1 and Rac control chemokine-promoted T lymphocyte adhesion mediated by the integrin alpha4beta1. *Mol Biol Cell*. 2005; 16:3223–3235. [PubMed: 15872091]
19. Korn T, Fischer KD, Girkontaite I, Kollner G, Toyka K, Jung S. Vav1-deficient mice are resistant to MOG-induced experimental autoimmune encephalomyelitis due to impaired antigen priming. *J Neuroimmunol*. 2003; 139:17–26. [PubMed: 12799016]
20. Weckbecker G, Bruns C, Fischer KD, et al. Strongly reduced alloreactivity and long-term survival times of cardiac allografts in Vav1- and Vav1/Vav2-knockout mice. *Transpl Int*. 2007; 20:353–364. [PubMed: 17326776]
21. Scott D, Addey C, Ellis P, et al. Dendritic cells permit identification of genes encoding MHC class II-restricted epitopes of transplantation antigens. *Immunity*. 2000; 12:711–720. [PubMed: 10894170]
22. Marelli-Berg FM, Peek E, Lidington EA, Stauss HJ, Lechler RI. Isolation of endothelial cells from murine tissue. *J Immunol Methods*. 2000; 244:205–215. [PubMed: 11033033]
23. James MJ, Belaramani L, Prodromidou K, et al. Anergic T cells exert antigen-independent inhibition of cell-cell interactions via chemokine metabolism. *Blood*. 2003; 102:2173–2179. [PubMed: 12775572]
24. Cinamon G, Shinder V, Alon R. Shear forces promote lymphocyte migration across vascular endothelium bearing apical chemokines. *Nat Immunol*. 2001; 2:515–522. [PubMed: 11376338]
25. Savinov AY, Wong FS, Stonebraker AC, Chervonsky AV. Presentation of antigen by endothelial cells and chemoattraction are required for homing of insulin-specific CD8+ T cells. *J Exp Med*. 2003; 197:643–656. [PubMed: 12615905]
26. Manes TD, Pober JS. Antigen presentation by human microvascular endothelial cells triggers ICAM-1-dependent transendothelial protrusion by, and fractalkine-dependent transendothelial migration of, effector memory CD4(+) T cells. *J Immunol*. 2008; 180:8386–8392. [PubMed: 18523306]
27. Mempel TR, Henrickson SE, Von Andrian UH. T-cell priming by dendritic cells in lymph nodes occurs in three distinct phases. *Nature*. 2004; 427:154–159. [PubMed: 14712275]
28. Michel F, Acuto O. CD28 costimulation: a source of Vav-1 for TCR signaling with the help of SLP-76? *Sci STKE*. 2002; 2002(144):PE35. [PubMed: 12165654]
29. Sechi AS, Wehland J. Interplay between TCR signalling and actin cytoskeleton dynamics. *Trends Immunol*. 2004; 25:257–264. [PubMed: 15099566]
30. Marelli-Berg F, Okkenhaug K, Mirenda V. A two-signal model for T cell trafficking. *Trends Immunol*. 2007; 28:267–277. [PubMed: 17481953]

31. Barreiro O, de la Fuente H, Mittelbrunn M, Sánchez-Madrid F. Functional insights on the polarized redistribution of leukocyte integrins and their ligands during leukocyte migration and immune interactions. *Immunol Rev.* 2007; 218:147–164. [PubMed: 17624951]
32. Jarmin SJ, David R, Ma L, et al. Targeting T cell receptor-induced phosphoinositide-3-kinase p110delta activity prevents T cell localization to antigenic tissue. *J Clin Invest.* 2008; 118:1154–1164. [PubMed: 18259608]
33. Woolf E, Grigorova I, Sagiv A, et al. Lymph node chemokines promote sustained T lymphocyte motility without triggering stable integrin adhesiveness in the absence of shear forces. *Nat Immunol.* 2007; 8:1076–1085. [PubMed: 17721537]
34. Chang TT, Jabs C, Sobel RA, Kuchroo VK, Sharpe AH. Studies in B7-deficient mice reveal a critical role for B7 costimulation in both induction and effector phases of experimental autoimmune encephalomyelitis. *J Exp Med.* 1999; 190:733–740. [PubMed: 10477557]
35. Girvin AM, Dal Canto MC, Rhee L, et al. A critical role for B7/CD28 costimulation in experimental autoimmune encephalomyelitis: a comparative study using costimulatory molecule-deficient mice and monoclonal antibody blockade. *J Immunol.* 2000; 164:136–143. [PubMed: 10605004]
36. Tiede I, Fritz G, Strand S, et al. CD28-dependent Rac1 activation is the molecular target of azathioprine in primary human CD4+ T lymphocytes. *J Clin Invest.* 2003; 111:1133–1145. [PubMed: 12697733]
37. Poppe D, Tiede I, Fritz G, et al. Azathioprine suppresses ezrin-radixin-moesin dependent T cell-APC conjugation through inhibition of Vav guanosine exchange activity on Rac proteins. *J Immunol.* 2006; 176:640–651. [PubMed: 16365460]

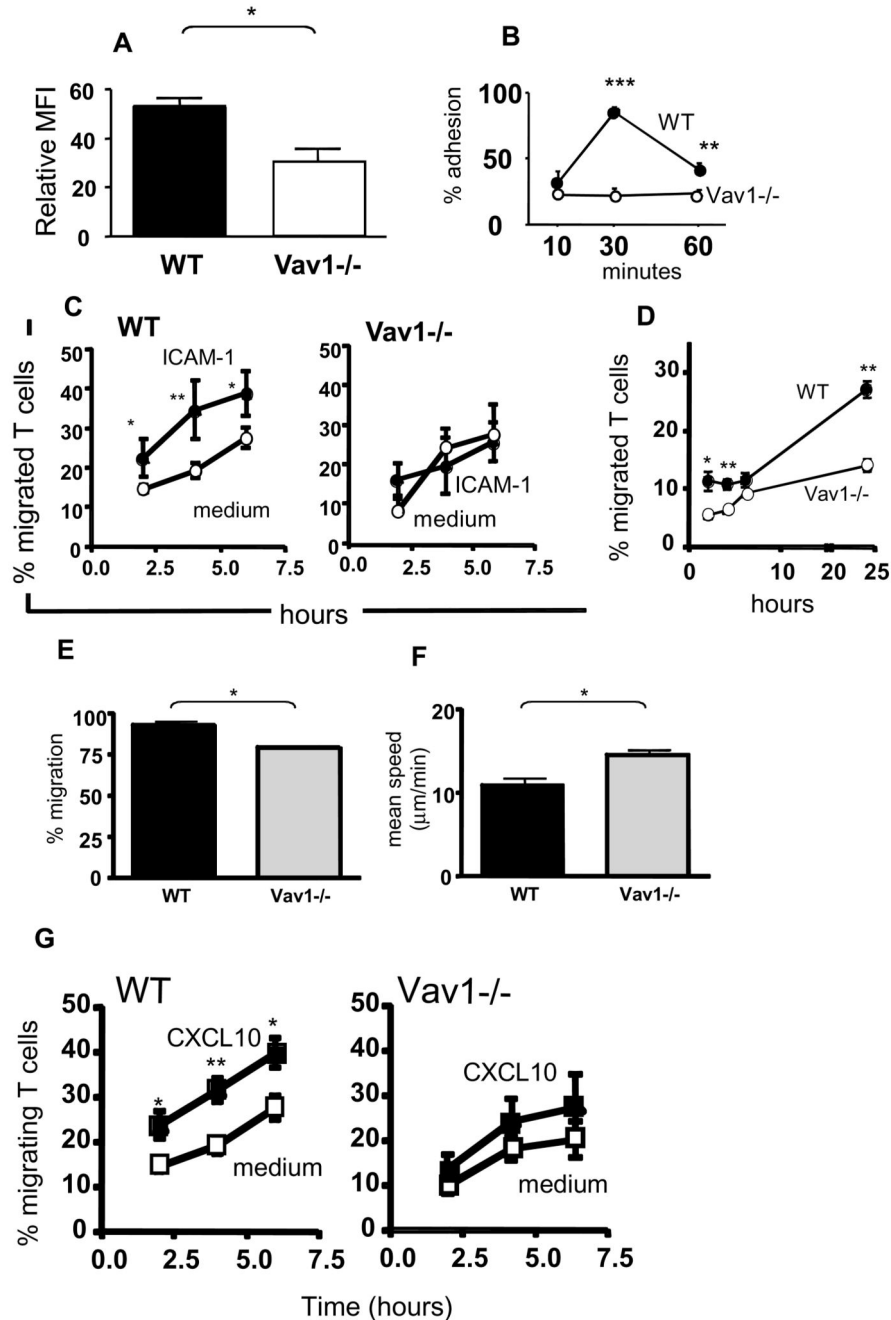


Figure 1. Motility of Vav1^{-/-} T cells *in vitro*.

Panel A: mean expression (from at least three independent experiments) of LFA-1 by HY-specific CD4⁺ WT and Vav1^{-/-} T cells seven days following antigen stimulation. Panel B: Mean adhesion (from at least three independent experiments) by WT and Vav1^{-/-} T cells to ICAM-1 (2 μg/ml)-coated 96-well plates at the indicated time points. Panel C: Mean migration (from four independent experiments) by WT and Vav1^{-/-} T cells 6 hours after plating onto ICAM-1-coated transwells. Panel D: Mean migration by WT and Vav1^{-/-} T cells through syngeneic female EC monolayers. Migration was measured at 2, 4, 6, and 24

hours. The percentage of migrated cells was calculated by dividing the number of cells in the bottom chamber by the total input of T cells from the mean of three experiments.

Panels E-F: Migration by WT and Vav1^{-/-} T cells plated on ICAM-1-coated dishes was analyzed by time-lapse microscopy. The number of cells migrating was quantified by counting motile T cells (E). T cells were tracked using Kinetiq tracking software and their migratory speed (F, $\mu\text{m}/\text{min}$) was quantified using Mathematica spreadsheets. The mean percentage of motile cells and mean speed was calculated from data of three independent experiments. Panel G: WT and Vav1^{-/-}-T-cell migration in response to CXCL10 through a transwell was assessed by counting the cells in the bottom chamber at 2, 4 and 6 hours. Percentage migration was calculated by dividing the number of cells in the bottom chamber by the original number of cells plated on the transwell. The mean percentage migration from four independent experiments is shown.

Error bars indicate standard error (* $p < 0.05$, ** $p < 0.01$, *** $p < 0.001$).

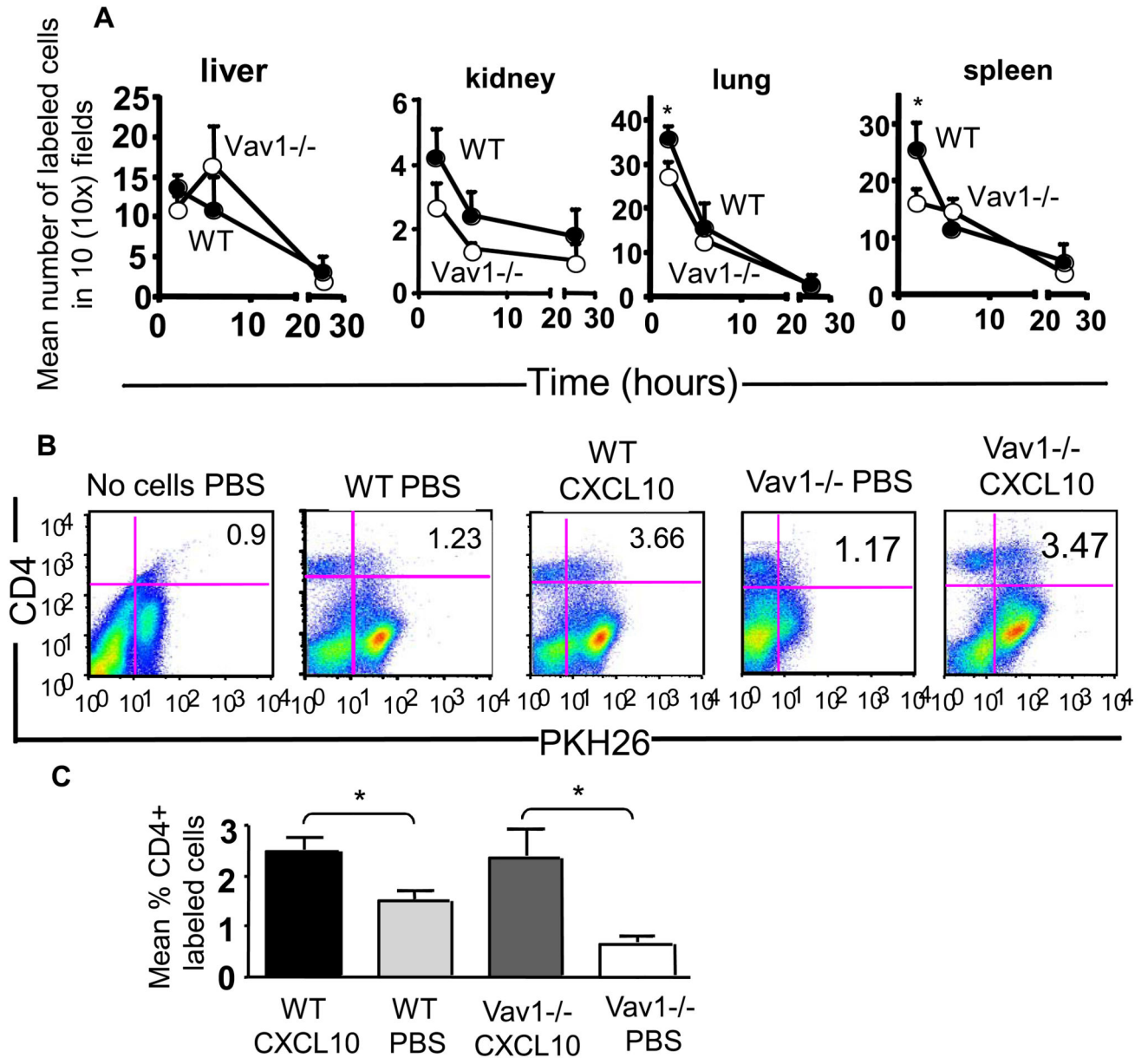


Figure 2. Constitutive and chemokine Vav1^{-/-} effector T-cell trafficking *in vivo*.

Panel A: HY-specific CD4⁺ WT and Vav1^{-/-} T cells were labeled with PKH26 (red) or CFSE (green) respectively and injected iv in syngeneic female mice. Trafficking into kidney, liver, lung and spleen was monitored at 2, 6 and 24 hours post-injection by harvesting, snap-freezing the tissue and taking 5-10 μ m sections. The mean number of cells from at least six tissue sections from at least three was quantified by wide-field fluorescence microscopy as described in Materials and Methods. Panels B and C: WT and Vav1^{-/-} T were labeled with PKH26 and injected iv into syngeneic female mice that had received an ip injection of 1.2 μ g CXCL10. Some mice were also injected with PBS alone (i.e. no T cells) as an autofluorescence control. Mice were sacrificed 16 hours later, and the presence of PKH26-labeled, CD4-positive T cells was analysed by flow cytometry. Representative dot plots are

shown in panel B. The mean percentage of cells present in the peritoneal lavage (calculated by subtracting the average background migration) from the percentage of migrated cells in the presence of CXCL10 is shown in panel C. Owing to the presence of an autofluorescent population of non-T cells often detected in FL-2 (also in control mice that received saline solution), cells were double-stained with an APC-conjugated anti-CD4 antibody following harvesting and the percentage of PKH26 (FL-2)-labeled T cells gated in the CD4⁺ T cell population is shown in the histogram and the graph representing cumulative data from at least three animals. The mean \pm SEM observed in samples from at least three animals are shown. Standard errors are shown (* $p < 0.05$).

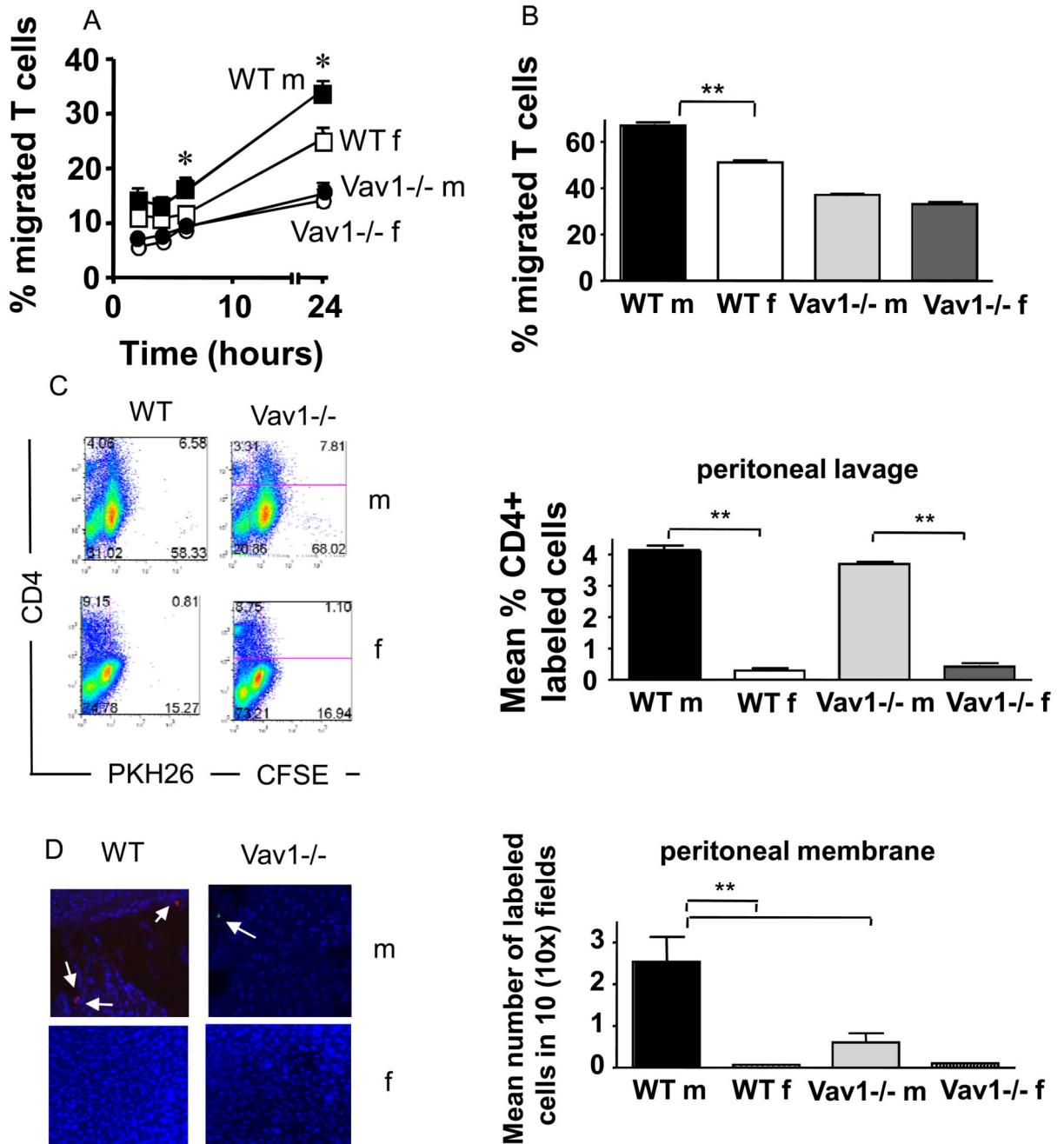


Figure 3. Antigen-driven Vav1^{-/-} T-cell migration.

HY-specific CD4⁺ WT and Vav1^{-/-} T cells (3×10^5) were seeded onto IFN γ -treated antigenic (male) or non-antigenic (female) syngeneic EC monolayers grown on transwells. The mean percentage migration at the indicated time points from three experiments of similar design is shown. Panel B: T cells (1×10^6) were plated on 35mm dishes coated with of IFN γ -treated antigenic (male) or non-antigenic (female) EC and allowed to migrate for 50 minutes. Pictures were taken every 30 seconds and analysed as described in Materials and Methods. Transmigrating T cells were defined as changing phase i.e. turning from bright to dark once

under the endothelial monolayer. Mean percentage of cells transmigrating was calculated from three independent experiments from a sample of 100 cells per movie.

Panels C-F: HY-specific CD4⁺ WT and Vav1^{-/-} T cells labeled with PKH26 (red) and CFSE (green), respectively were co-injected iv into syngeneic male or female recipients which had previously received an ip injection of IFN γ . Labeled T-cell enrichment into the peritoneal lavage was analysed by flow cytometry 24 hours later (C). The mean percentage of CD4⁺ labeled (PKH26 or CFSE) T cells in the peritoneal lavage from at least three animals is shown (D). Nuclei are stained by DAPI (blue). Retention of T cells into the peritoneal membrane (panel E) was analysed by wide-field fluorescence microscopy as described in the legend to Figure 2. The mean number of cells in six tissue samples from at least three mice is shown (panel F).

Error bars indicate standard error of the mean (*p<0.05, **p<0.01).

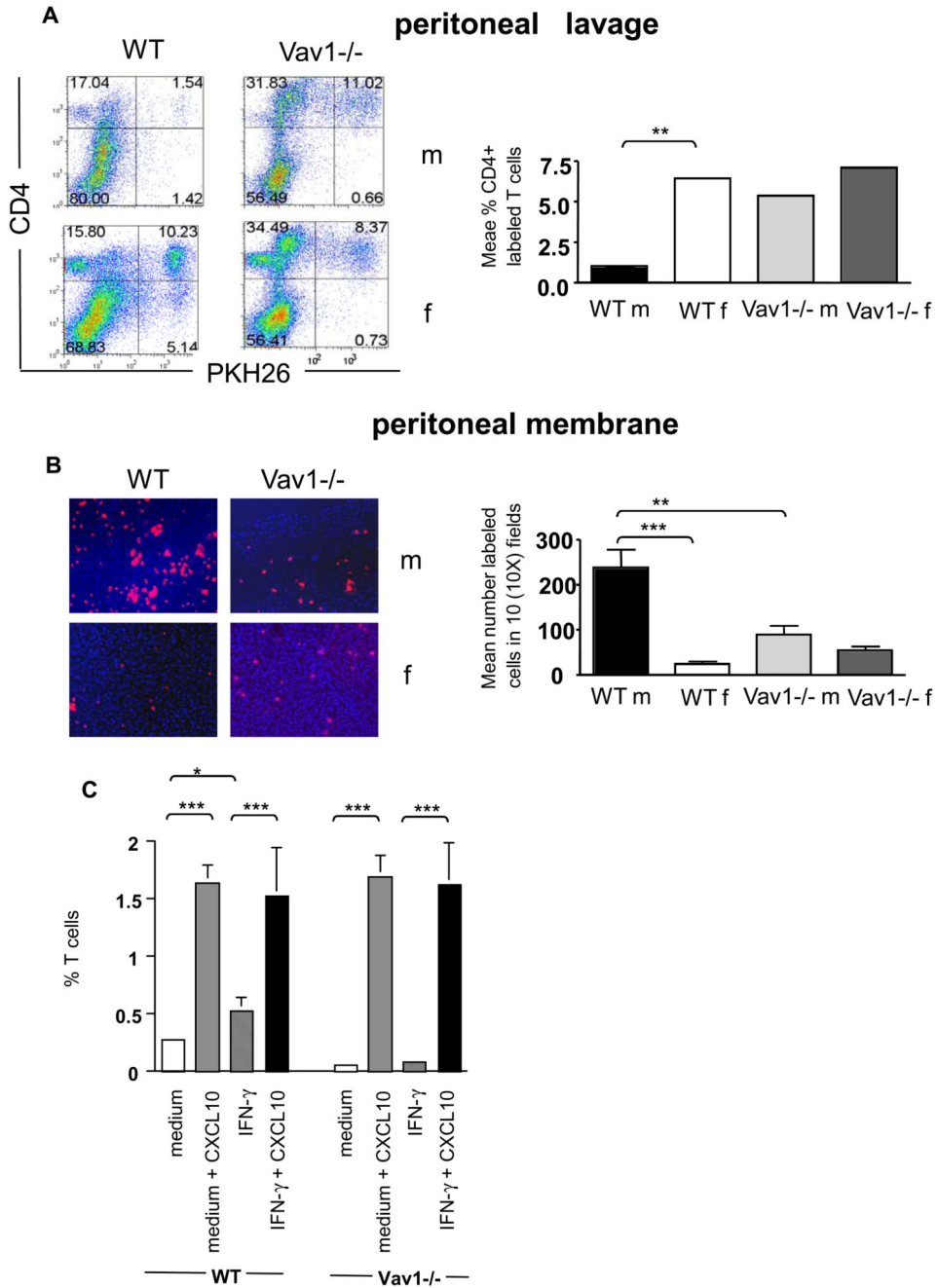


Figure 4. A combination of shear flow and chemokines sustains Vav1^{-/-} T-cell migration. Panels A-B: PKH26-labeled HY-specific CD4⁺ WT or Vav1 T cells (3×10^6) were injected ip in syngeneic male mice that had previously received an ip injection of IFN γ to induce MHC class II expression and antigen presentation. The percentage of T cells remaining in the peritoneal cavity and T-cell infiltration of the peritoneal membrane were evaluated 24 hours later by flow cytometry and wide-field fluorescence microscopy, respectively, as described in the legend to Figure 2. Representative examples of peritoneal lavage dot plots and peritoneal membrane sections (x10 magnification) are shown. The mean number of cells in

the peritoneal membrane and lavage from at least four mice are shown. Error bars indicate standard error (* $p < 0.05$, ** $p < 0.01$).

Panel C: HY-specific WT and *Vav1*^{-/-} CD4⁺ T cells were perfused at 37 °C over male-derived EC-coated slides at a fixed shear stress of 2.5 dynes/cm² for 10 minutes. Some EC were pre-treated with IFN γ for 48 hours to induce antigen presentation (indicated as IFN γ , panel C). In some experiments, ECs were overlaid with CXCL10 (300 ng/ml) for 2 hours prior to use in the flow assay. Slides were then removed, gently washed with warm PBS and exposed to 0.05% trypsin-EDTA solution to obtain a cell suspension. The number of labeled T cells in this suspension was evaluated by flow cytometry (by gating on the small lymphocyte population and comparing the number of green- and red- fluorescent cells). The graphs summarize data obtained from at least three experiments. Error bars are shown (* $p < 0.05$, ** $p < 0.01$).

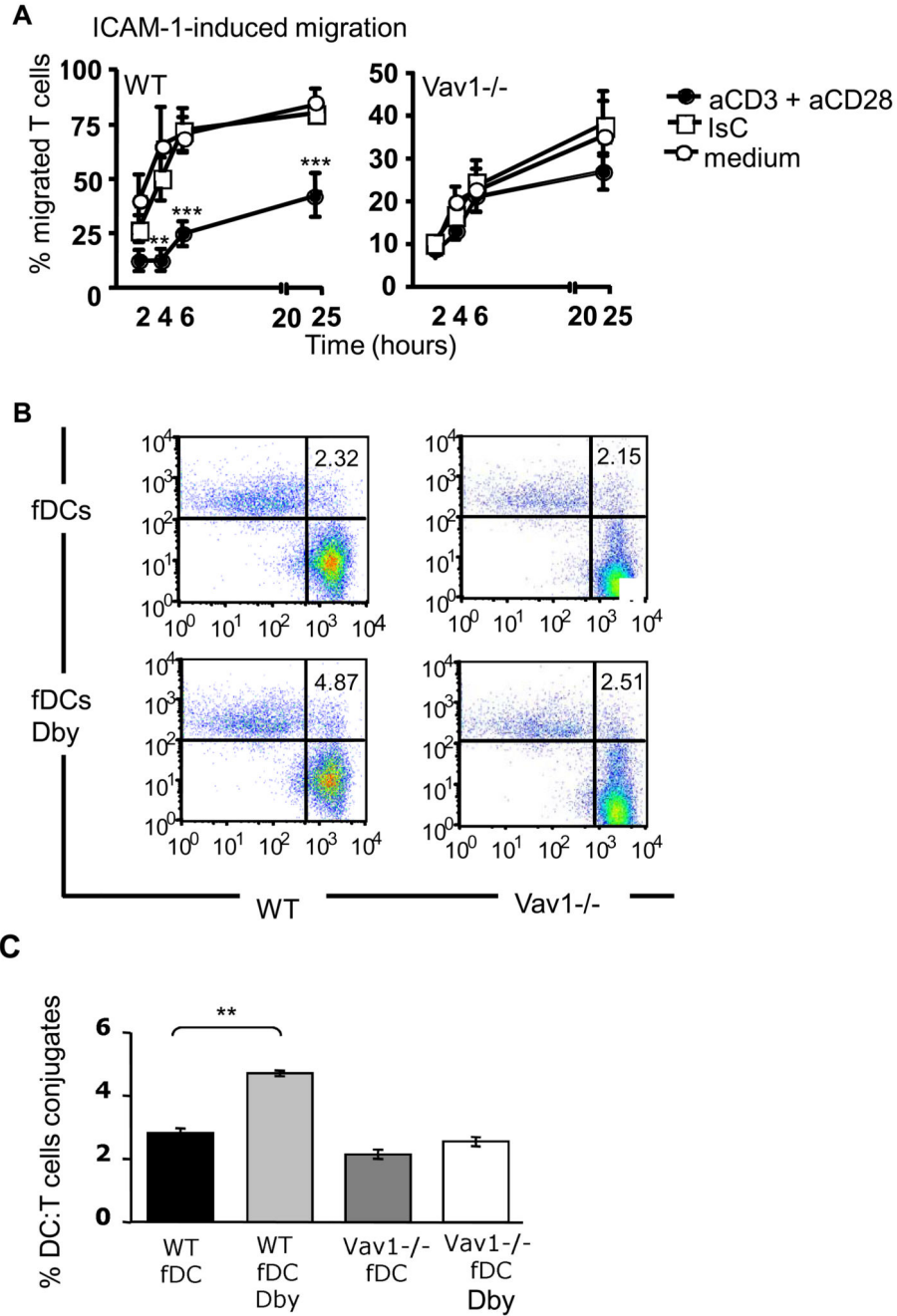


Figure 5. Vav 1^{-/-} T cells are not susceptible to antigen-induced stop signals.

Panel A: HY-specific A^b-restricted WT and Vav1^{-/-} T were incubated with plastic bound anti-CD3 and anti-CD28 for 45 minutes and plated on rICAM-1-coated transwells. As a control, T cells were exposed to hamster Ig isotype control or medium alone. Migration was measured as indicated in the legend to Figure 1. The percentage of migrated cells was calculated by dividing the number of cells in the lower chamber with the number of cells plated on the traswells. Error bars indicate standard error (** p<0.01, ***p<0.001).

Panel B: DCs were obtained from bone marrow of syngeneic female mice (fDCs) and cultured for 7 days in GM-CSF, followed by overnight LPS-induced maturation. HY-specific A^b-restricted CD4⁺ PKH26-labeled WT or Vav1^{-/-} T cells were incubated with CFSE-labeled female-derived DCs pulsed with 50nM Dby peptide for 2 hours (fDCs Dby). Non-antigenic DCs (fDCs) were used as a control. Conjugate formation was analysed by flow cytometry as described in Materials and Methods. The mean percentage of conjugate formation from four experiments is shown in panel C. Error bars indicate standard error (**p<0.01, ***p<0.001).

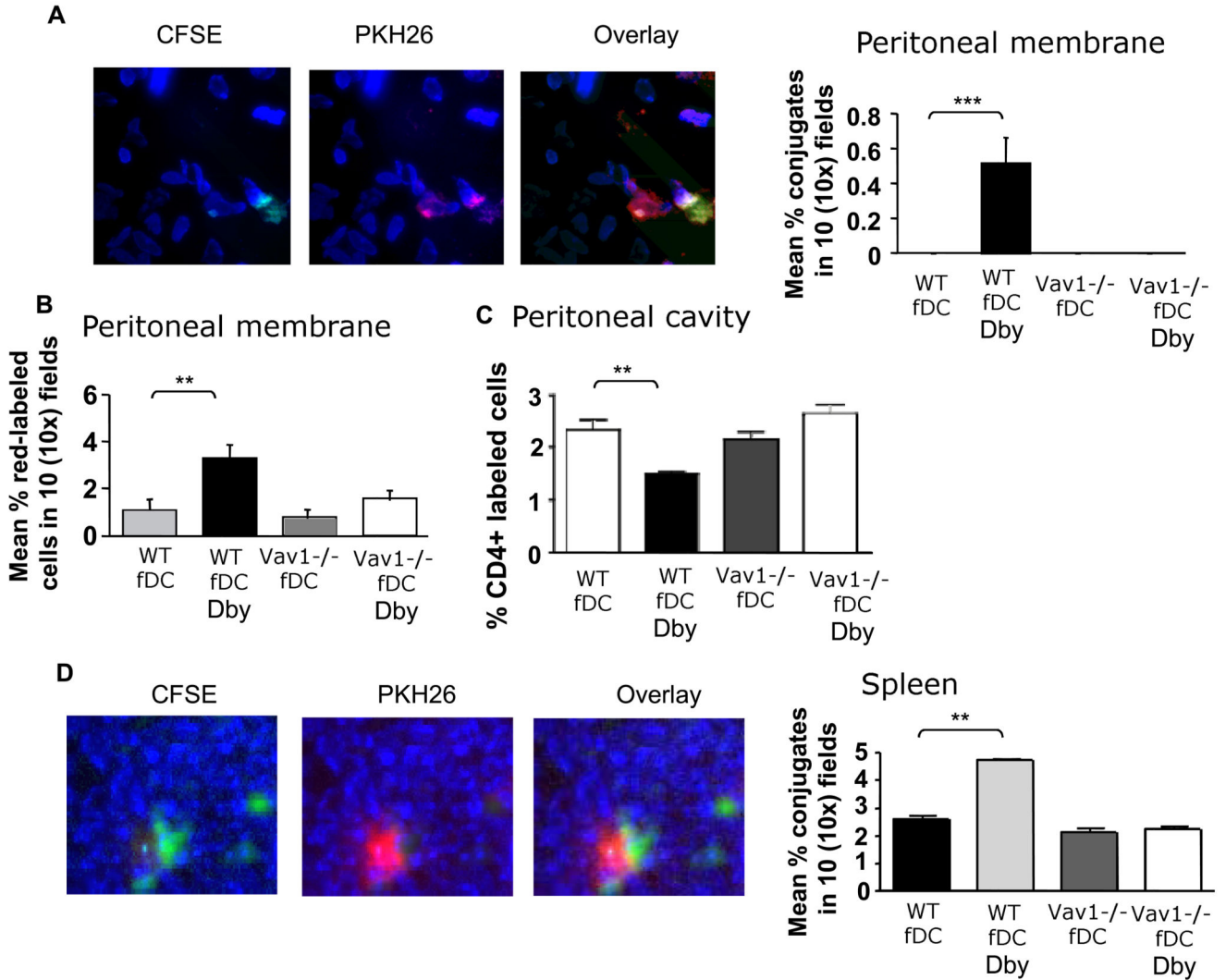


Figure 6. Vav1^{-/-} T cells display defective T cell: antigen presenting DC interactions *in vivo*.

Panel A: 10^7 PKH26- labeled T cells were injected iv in syngeneic female mice that simultaneously received an ip injection of Dby-peptide pulsed female-derived matured DCs labeled with CFSE, or DCs alone as a control. HY-specific CD4⁺ WT and Vav1^{-/-} T cells and DCs were injected alone as a control. In this model, T cells travel into the bloodstream and reach the peritoneal membrane and the spleen, whereas DCs travel out of the peritoneal cavity, through the peritoneal membrane, enter the bloodstream and reach the spleen. The presence of T-cell: DC conjugates in the peritoneal membrane and spleen was quantified 24 hours later by wide-field fluorescence microscopy as described in Materials and Methods. The occurrence of cell:cell interactions was apparent as yellow fluorescence. Representative 40x images from the peritoneal membrane (A) and the spleen (D) are shown. The number of conjugates in the peritoneal membrane (A) and spleen (D) were averaged and quantified with the algorithm described in Materials and Methods in ten 10x images obtained from samples from at least six animals. In addition, the mean number of labeled T cells (not engaged by DCs) in the peritoneal membrane and cavity was measured as

described in the legend to Figure 3, and is shown in panels B and C, respectively. No T cells:DC conjugates were detected in the peritoneal lavage (data not shown). Error bars indicate standard error (** $p < 0.01$, *** $p < 0.001$).

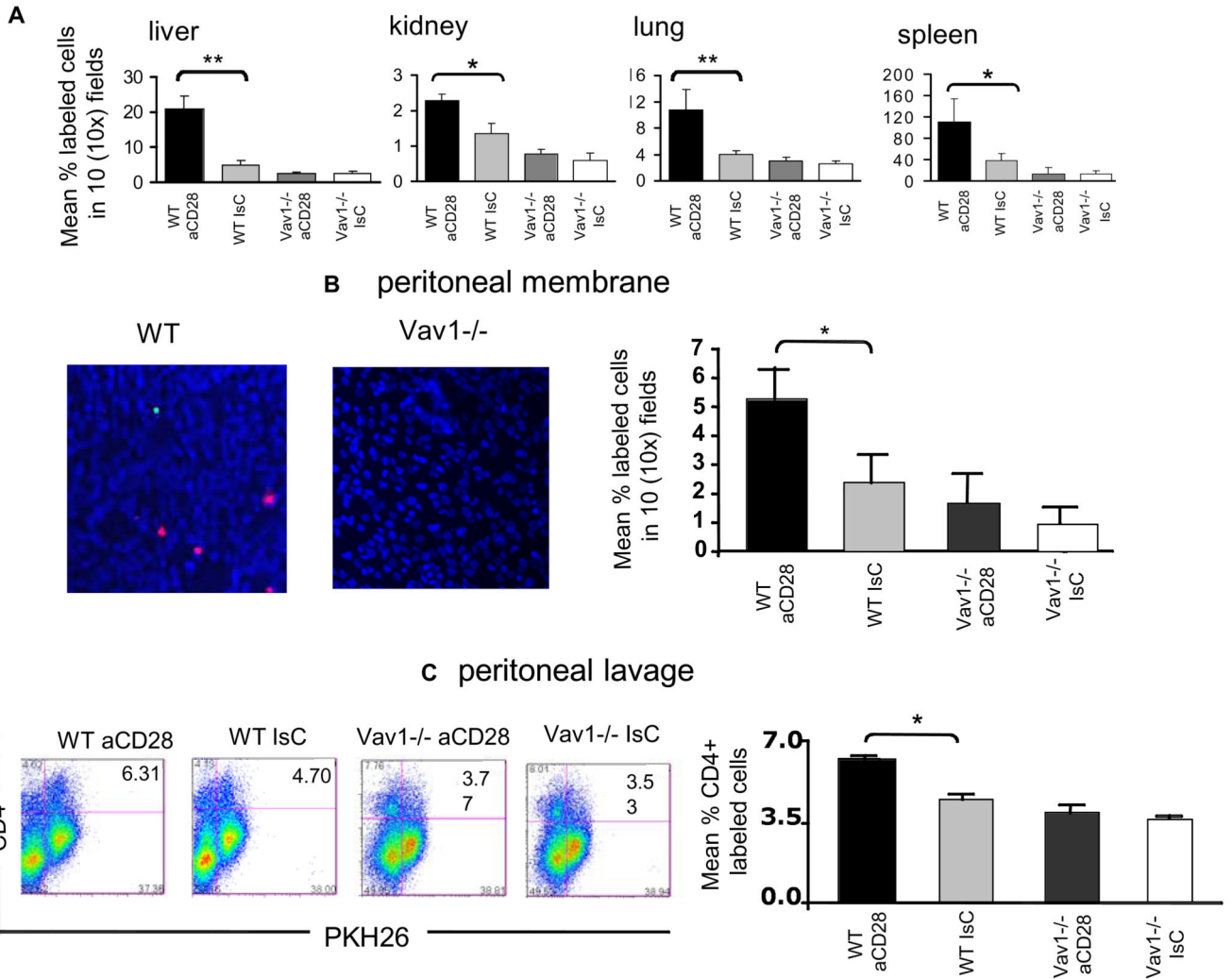


Figure 7. Vav1^{-/-} - cell motility is not susceptible to CD28-mediated regulation.

Panel A: HY-specific CD4⁺ WT and Vav1^{-/-} T cells which had either undergone antibody-mediated CD28 ligation (30 minutes at 37°C, PKH26-labeled) or had been pre-treated with an antibody isotype control (CFSE-labeled) were injected iv (10^7 /mouse) into syngeneic female recipients. The presence of fluorescently labeled cells in the indicated organs was assessed 24 hours later as described in the legend to Figure 2. The mean T-cell number \pm SEM observed in samples from at least six animals are shown (* $p < 0.05$, ** $p < 0.01$).

Panel B-C: HY-specific CD4⁺ WT and Vav1^{-/-} T cells, which had either undergone antibody-mediated CD28 ligation (PKH26-labeled) or had been pre-treated with an antibody isotype control (CFSE-labeled) were injected iv (10^7 /mouse) into male mice that had received an ip injection of IFN γ 48 hours earlier. The presence of fluorescently labeled cells in the peritoneal membrane (B) and cavity (C) was assessed 24 hours later as described in the legend to Figure 3. The mean T-cell number \pm SEM observed in samples from at least three animals is shown in the right-hand side panels (* $p < 0.05$, ** $p < 0.01$).